Spatial analysis of eroding surface micro-topographies

Ritienne Gauci [a], Rob Inkpen [b,*], Philip J. Soar [b]

[a] *Department of Geography, University of Malta, Tal-Qroqq, Msida, MSD 2080, Malta*
[b] *School of the Environment, Geography & Geosciences, University of Portsmouth, Portsmouth, UK*

ARTICLE INFO

ABSTRACT

Analysis of the spatial variability in erosion rates at the micro-scale has the potential to improve our understanding of how shore platforms erode. Comparing the erosion rate of a single measurement reading with the erosion rate of other increasingly distant readings would indicate whether average variation in erosion rate is homogeneous and at what spatial scale. Little variation in erosion rate from one measurement reading as distance increased would indicate that an area is eroding homogeneously and that the surface measured is responding as a single spatial unit. An increase or decrease in the variation in erosion rate difference with increasing distance from one reading would suggest that the area was not acting as a single spatial unit and that surface responses differ with scale. This study used a two-year dataset of traversing micro-erosion meter (TMEM) readings, collected from two limestone shore platforms on the north of Malta, at Ponta tal-Qammieħ and Blata l-Bajda, in order to explore the relationship between difference in erosion rate and distance from TMEM readings. A Microsoft Excel macro was developed and applied to calculate and analyse the average variation in erosion rate difference between all possible pairs of measurement readings over a set of fixed distances. The resultant analysis suggests that there are some consistent patterns between measurement periods and locations on a platform in terms of how erosion rate difference varies with distance between readings. These are not simple relationships to either characterise or explain but nevertheless, they suggest variations in how the same surface responds to erosional forces. These findings are significant for erosion research as they imply that spatial scales to erosion within even small areas may impact upon the representativeness of an average erosional loss for the platform site. It raises issues about how representative rates really are and contributes to the discussion about the wider understanding of erosion rates across spatial scale.

1. Introduction

Erosion of rock surfaces produces micro-topographies that vary across a range of spatial and temporal scales. Identifying and quantifying changes in surface topography are critical for identifying associations between processes, spatio-temporal dimensions and surface erosion (Stephenson and Kirk, 1998; Inkpen et al., 2004; Inkpen and Stephenson, 2006; Inkpen et al., 2010; Porter et al., 2010a; 2010b; Stephenson et al., 2017; Yuan et al., 2020). On shore platforms, the quantification of erosion has often involved investigations at relatively short-term temporal scale (from decadal to hourly) and small spatial scale (from centimetre to sub-millimetre) with the use of instruments such as the micro-erosion meter (MEM) and its variant, the traversing micro-erosion meter (TMEM) (Stephenson and Kirk, 1998; Stephenson and Finlayson, 2009; Moses et al., 2014).

The use of T/MEM across a range of spatial and temporal scales has

contributed to better quantify the variable rates of rock surface change, the latter long associated with an array of processes operating in a range of boundary conditions such as oceanic and non-oceanic coasts, different lithologies, tidal regime and elevations (Yuan et al., 2022). However, the contribution of each single process is not an easy one to unpack, due to potential inter-connectivity between different mechanisms (Viles, 2013) or how processes scale over longer timeframes and larger space dimensions (Turowski and Cook, 2017; Yuan et al., 2022). Alternative approaches to T/MEM data modelling and analysis are therefore required in order to capture better the behaviour and trends of such rates over space and time. The approaches may also build on the new body of knowledge being generated through other techniques such as Structure for Motion (SfM), the later used to assess the relationship between the nature of erosion (by surface detachment) and surface micro-topographies, and which in turn depends on the micro-structure of shore platforms (Swirad et al., 2019).

The conventional approach adopted in most MEM studies has been to focus on measuring trends of temporal changes in erosion rather than spatial changes within each bolt site, given the relatively small spatial scale of each bolt site (c. 50cm^2) and the limitation in sample size of readings per bolt site. On the other hand, though a TMEM provides numerous individual readings at each bolt site, these readings were commonly aggregated into one single mean value of erosion rate (Stephenson and Finlayson, 2009). Often, the assumption was that regardless of its uneven micro-topography, the selected bolt sites were representative of the surface characteristics of the wider shore platform, especially when the network of bolt sites followed a cross-shore direction (Yuan et al., 2022). Thus, when spatial variations in erosion rates were examined and compared between bolt sites, they were assumed to be related to the variation in processes experienced more broadly across

a shore platform progressing from the seaward to landward sides.

The aggregation of readings into single annual erosion rates was often found to also underrepresent surface swelling events which were induced by short-term or seasonal micro-climatic variables (such as temperature, humidity, hours of sunlight) or biological activity (e.g. colonised biofilms) over hours to days (Mottershead, 1989; Stephenson and Kirk, 2001; Stephenson et al., 2004; Gómez-Pujol et al., 2007; Porter et al., 2010a, b; Mayaud et al., 2014; Yuan et al., 2018, 2019). Knowledge of the spatial variability between rates of surface rises and those of surface lowering within each bolt site may therefore contribute to better define the behaviour of surface change, especially on supratidal surfaces where erosion rates were observed to be widely variable, even when considering the lithologically similar rocks such as limestone (Torunski, 1979; Shakesby and Walsh, 1986; Moses et al., 2015).
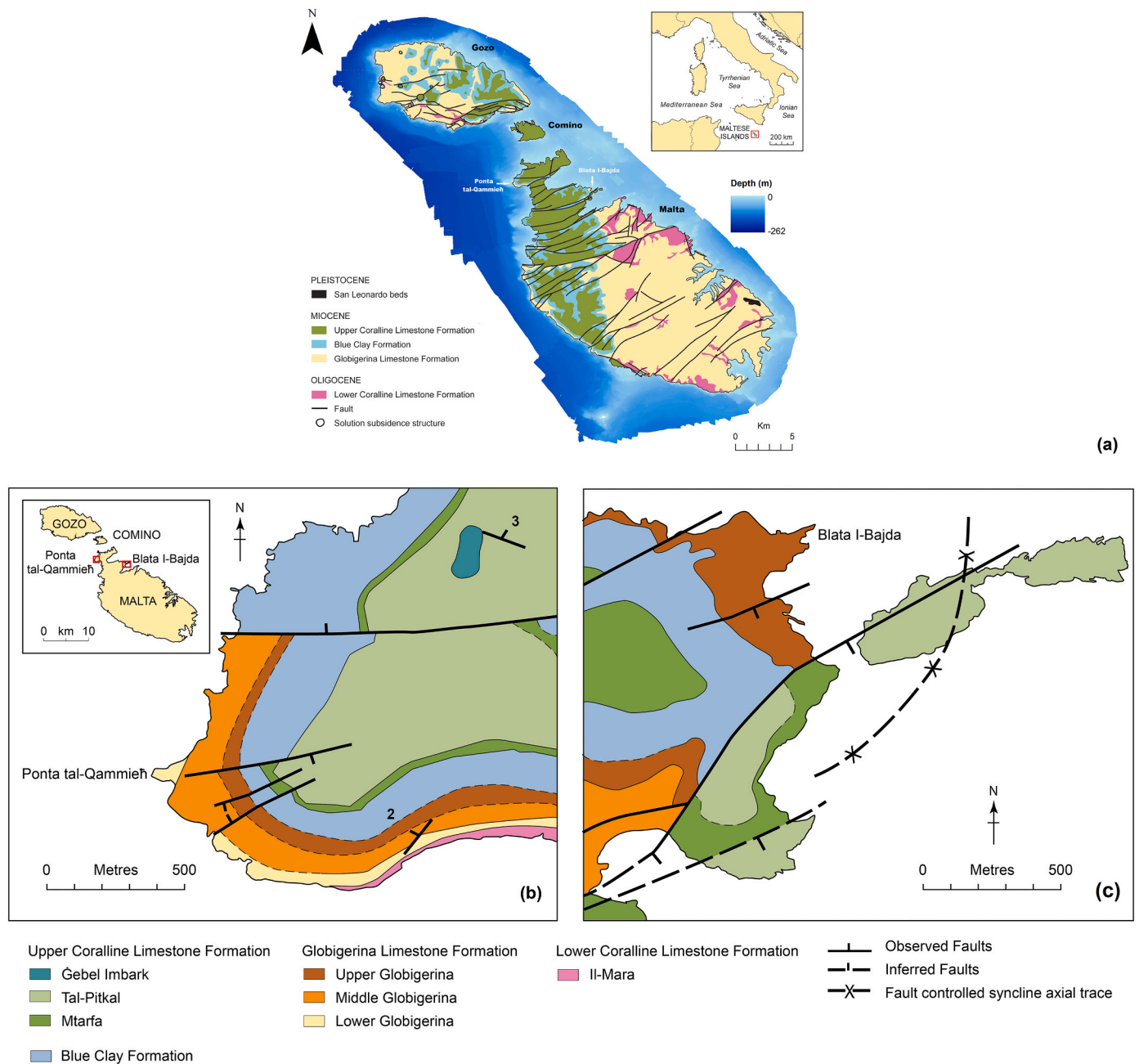

Fig. 1. a. Geology and bathymetry of the Maltese Islands and location of selected shore platform sites. (Source: Geological map redrawn from Oil Exploration Directorate, 1993; Bathymetric map from ERDF LIDAR data, 2012); b. Detailed Geology of Blata l-Bajda area; c. Detailed Geology of Ponta tal-Qammieħ area (Source: Geological map redrawn from Oil Exploration Directorate, 1993).

This paper investigates the spatial variability of erosion rates within TMEM bolt sites at supratidal levels on two limestone shore platforms on the north of Malta (Fig. 1), by comparing how differences in average erosion rates vary between reading points as the distance between points increases. We define and apply a measure of spatial autocorrelation, similar to the semivariogram, to explore if there is a consistent relationship and examine whether any identified spatial trends relate to the underlying micro-topography of the bolt sites. This alternative statistical approach allows for a better understanding of how well the rates and mode of surface change within each bolt site are representative of the nature of erosion of a platform site.

Whilst it is expected that the rate of change from one individual point to another may vary, the underlying assumption is that, as a collective, the individual changes will provide a good representation of the average change at the bolt site. In other words, the collective set of individual point data will provide an average change for the bolt site that masks the vagaries of variability of an individual point measurement. For measurement and analytical purposes, each individual point is considered to be independent of all the other points within the bolt site. Implicitly, variation in scale is assumed only to occur at the level of the individual point. In reality, researchers cannot exclude the possibility that points on the measured surface at each bolt site may be influenced by the same erosion processes and, if the topography is appropriate, loss at one point on a slope may accumulate elsewhere at the base of the slope. In other words, there is the hypothesis that change at one point within the bolt site may be related to change at others points in the bolt site.

Some researchers have grappled with this issue (e.g. Inkpen et al., 2004; Inkpen et al., 2010), but there is still relatively little exploration of the potential of TMEM data to identify and understand spatial variability within bolt sites. The recent development of methods such as laser scanning and SfM, it could be argued, have made such exploration redundant as such methods extent monitoring capabilities to thousands, if not millions of data points, across a surface. However, the key issues of how to interpret individual as opposed to a collection of data points remains as does the issue of interdependence between data points. Understanding scale in spatial variation of erosion rates is still an issue.

2. Theoretical background

Substantial literature on erosion of shore platform measured by T/MEM has been generated for the infralittoral zone along oceanic coasts (Stephenson and Finlayson, 2009). Recently, there has been a growth in the number of studies about rates of surface change on supratidal platform surfaces, some of which belonged to non-oceanic coasts and which are governed by a micro-tidal regime of semi-enclosed seas such as the Mediterranean (Swantesson et al., 2006; Gómez-Pujol et al., 2006; Andriani and Walsh, 2007; Furlani et al., 2009; Furnali et al., 2011; Furlani et al., 2014; Chelli et al., 2010; Chelli et al., 2012; Pomar et al., 2017; Pappalardo et al., 2017; Gauci, 2018 and references therein).

The extent and magnitude of mechanical wave action on supratidal platforms would be determined by a number of factors such as: force of the storm waves, water depth at which storm waves will break, platform seaward morphology and its elevation beyond high tide. Studies have observed how wave action on sub-horizontal platforms with a micro-tidal regime is largely concentrated along seaward scarp edge due to shoaling and refraction (Stephenson, 1997; Stephenson and Kirk, 2000a; Marshall and Stephenson, 2011). Water shock, water hammer, air compression and wave dissipation are infrequent and storm episodic in a cross-shore direction (Stephenson and Thornton, 2005).

The influence of water-layer weathering on platform surface lowering rates was relatively more observed and measured on intertidal platforms than on supratidal surfaces (Trenhaile, 1987; Stephenson and Kirk, 2000b; Kanyaya and Trenhaile, 2005; Porter et al., 2010b; Mottershead, 2013;). The role of wetting and drying is less regular and effective at supratidal conditions, especially on sub-horizontal platforms bounded from the intertidal zone by a vertical seaward scarp and those limited by a micro-tidal regime. However, this does not mean that such a mechanism is completely absent from supratidal zones. Stephenson and Kirk (2005) reported that it can occur up to 24 m above sea level where sea spray accumulates. Wetting and drying processes in these zones would be driven by seasonality such as episodic wetting by wave splash during heavy seas and by rainfall, which all lead to slaking form of rock breakdown (Mottershead, 1989; Kanyaya and Trenhaile, 2005; Mottershead, 2013).

Zonation of weathering forms has also been reported on limestone supratidal platforms, with alveoli and fretted hollows mostly developed in the front spray zone and solution and pits mostly located in the landward part of the platform (Moses and Smith, 1994). Such zonations confirm a cross-shore component in how the susceptibility to weathering system spatially operates in relation to the land-sea water interface. Limestone shore platforms are not only characterized by a large variety in morphology, but also by highly heterogeneous surface change dynamics at micro-scale. Inkpen et al. (2010) concluded that limestone coasts do not display a consistent mode of surface change, both over the short- and long-term scales. Mayaud et al. (2014) claimed that petrographic variations within the limestone could lead to differential responses to insolation, both at the surface and inside the rock mass. Erosion rates were reported to be widely variable within the supratidal zone, even when considering the lithologically similar rocks such as limestone (Torunski, 1979; Shakesby and Walsh, 1986; Swantesson et al., 2006; Moses et al., 2015).

Rock surface behaviour was also observed to be complex at different temporal scales from hours to multiple days, with recorded cycles of expansion and contraction and spatial heterogeneity driven site-specific conditions. Yuan et al. (2018) noted how two-hourly surface changes (driven primarily by humidity and temperature micro-conditions) were also characterized by spatial heterogeneity, with contraction and expansion occurring concurrently at centimetre scale across the rock surface in three distinct periods of rising (morning), falling (afternoon and evening) and stable (night).

An array of biogeomorphic processes have also been recognised to be partially responsible for cyclic behaviour in rock surface change and noted for their efficacy on sedimentary surfaces such as limestone and sandstone (Moses and Smith, 1994; Spencer and Viles, 2002; Carter and Viles, 2005; Gómez-Pujol et al., 2006; Viles et al., 2008; Naylor et al., 2012; Moses, 2013; Furlani et al., 2014; Mayaud et al., 2014; Yuan et al., 2018, 2019). Site-specific conditions influence rates of biological weathering on platform surfaces since it is governed by factors including zonation of organisms and sensitivity to moisture availability, tidal characteristics, temperature gradients, degree of exposure to sunlight and water salinity (Trenhaile, 1987). At supratidal levels, recent studies have elucidated how biological activity also contributed to short-term surface change. Gómez-Pujol et al. (2007) suggested how hourly surface changes on a supratidal cliff face may be caused by the expansion and contraction of lichen thalli, due to absorption of moisture and drying out of the cliff surface. Yuan et al. (2019) published lab experiments on supratidal sandstone surfaces which concluded that biofilms presence increased the magnitude and number of cycles of expansion and contraction and this may accelerate granular disintegration and rate of breakdown of supratidal rocks. A similar investigation by Mayaud et al. (2014) on a coastal supratidal limestone in France revealed surface change related largely to insolation in the morning and evening when thermal gradients were steepest and how the presence of a biofilm intensified rock expansion, but delayed surface response to microclimatic variability.

Preferential responses to specific micro-conditions may also determine spatial presence of biological agency on platform surfaces. Pomar et al. (2017) showed how limestone biopits on supratidal platforms were mostly distributed in shaded exposures and sheltered areas, away from prevailing winds and waves, direct insolation and desiccation. These studies continue to confirm the extent to which processes on supratidal limestone platforms can be both site-specific and temporally dependent.

Internal variability of erosion rates within a bolt site are often assumed to be relatively insignificant, yet identifying and exploring intra-site spatial variability permits an understanding of how well the average erosion rate is representative of the nature of erosion at a platform site. It also offers potential for the classification of platform sites according to different modes of erosion as it varies over a range of spatial scales (Inkpen, 2007). Identifying the nature of this intra-spatial variability and recognizing its potential change with physical setting and conditions over a platform surface allows for a more nuanced interpretation of erosion rates across the shore platform.

3. Geomorphology of shore platforms on the Maltese Islands and study areas

3.1. Physical setting

The Maltese Islands (Malta, Gozo and Comino) occupy a land surface of only 365 km^2 but have a long coastline of 272 km, with 97% of it comprising a diverse assemblage of limestone landforms (Gauci and Schembri, 2019). Despite Malta having the longest percentage length of 'rocky' coastline in the Mediterranean region (Woodward, 2009; Said and Schembri, 2010; Gauci and Schembri, 2019), the number of studies on erosional processes on Maltese shore platforms is still scant (Gauci, 2018 and references therein). With the use of a rock profiler, Micallef and Williams (2009) suggested high variability in erosion rates on selected Maltese shore platforms; however, the research was limited to analysing mean erosion rates at each site over the whole study period without focusing on the variability of erosion rates at an intra-spatial scale. In addition, the erosional behaviour of supra-tidal platform surfaces within a micro-tidal regime is not yet fully understood, not only in the Mediterranean region but also worldwide (Gauci, 2018).

Biolchi et al. (2016) estimated that 15% of Malta's coastline consists of shore platforms, generally described as near-horizontal surfaces with an abrupt low seaward terminus and deeply carved abrasional notches at mean sea level (Gauci, 2018; Gauci and Inkpen, 2019). Due to Malta's micro-tidal regime of only 0.206 m for spring tides and 0.046 m during neap tides (Drago, 2009), the vertical extent of the platforms' intertidal zone is limited and most shore platforms have surfaces permanently exposed at supratidal elevations of between 1 and 10 m. Some review studies on Maltese coastal landforms consider them as 'contemporary' shore platforms, i.e., platforms that were probably initiated at the beginning of the Holocene stillstand and thus have developed since the sea reached its present level about 6000 to 7000 years BP (Said and Schembri, 2010; Biolchi et al., 2016).

The Maltese archipelago consists of a horizontally stratified sequence of Oligo-Miocene limestones and marls and are intersected by two sets of faults trending in a NE-SW and NW-SE orientation from the early Miocene (23–16 Ma) and Pliocene (5.3–1.8 Ma), respectively (Fig. 1a). As a result of tectonic upwarping and rifting, a series of headlands and bays (and rias) were formed along the coast. A north-east structural tilt elevated the western and southern coasts of the island of Malta, revealing vertical or scree-sloping cliff faces with fully exposed stratigraphic sequences, and dipped most of the north-eastern and eastern coasts as low sloping profiles in Globigerina Limestone (GL) and Lower Coralline Limestone (LCL) (Alexander, 1988; Pedley, 2011; Galea, 2019; Gauci and Scerri, 2019).

Shore platforms in Malta mostly develop where the sub-horizontal layer of GL outcrops at sea level. Their genesis is mostly associated with differential erosion produced by wave action between three different lithological members present in the GL stratigraphy: (i) an uneven horizontal sequence of yellow calcareous limestone (Lower Globigerina Limestone, LGL); (ii) thick sections of grey limestone and marly limestone in the mid-section of the cliffs (Middle Globigerina Limestone, MGL); (iii) thinner inter-bedded strata of yellow calcareous limestones and greyish limestone marls (Upper Globigerina Limestone, UGL) (Paskoff and Sanlaville, 1978). MGL is a marly unit and its rapid

recession often exposes the harder surfaces of the underlying LGL as shore platforms at sea level.

3.2. Shore platforms at Blata l-Bajda and Ponta tal-Qammieħ

The selected platforms at Blata l-Bajda (35°58′02.82″N, 14°23′45.43″E) and Ponta tal-Qammieħ, (35°58′16.70″N, 14°19′23.56″E) represent two diverse geological sites, located on the north-eastern and north-western coasts, respectively (Fig. 1b and c).

The shore platform of Blata l-Bajda is situated within the coastal area of Selmun, north-eastern Malta (Fig. 1). The coastal geology and topography of Selmun are closely linked to the tectonic dynamics of the Great Fault, the latter responsible for a ridge-trough sequence consisting of Bajda Ridge, the Miżieb syncline (depression), the Mellieħa Ridge and part of the Mellieħa Valley (Fig. 3a). The shore platform of Ponta tal-Qammieħ is situated on the north-western point of Marfa Ridge (Malta) and is located in Mellieħa (Fig. 1). The site also falls to the north of the Great Fault which positioned Marfa Ridge as the last ridge on the island of Malta. Marfa Ridge was elevated by the tectonic uplift of the Pantelleria Rift system and as a result exposed the whole stratigraphic sequence of the Maltese lithology (Gianelli et al., 1972; Baldassini et al., 2013). A main W-E fault slices through Marfa Ridge (Fig. 1b) and lifting the Qammieħ area to be the highest part of the Marfa Ridge (129 m asl).

The shore platforms at Blata l-Bajda have developed from UGL stratigraphy and is considered to be the most extensive platform formed in UGL on the archipelago (Fig. 3a). UGL is subdivided into a sequence of four beds of variable lithological resistance to erosion from base to top as follows: (i) a relatively hard bed consisting of a C2 phosphorite pebble bed known as Upper Conglomerate bed; (ii) an overlying yellow-to-orange hard and compact limestone (Fig. 3b and c); (iii) the middle bed is formed by a calcareous mudstone in soft grey marl (Fig. 3b); (iv) a yellow-to-orange hard and compact limestone at the top of the sequence. In situations where the C2 pebble bed and the overlying compact yellow bed are located at sea level, they are more resistant to erosion than the overlying grey mudstone, typically resulting in a shore platform which develops at the base of the overlying retreating grey mudstone (Gauci and Inkpen, 2019). The visible part of this platform measures c. 120 m (of maximum length) by 30 m (of maximum width) and has a surface area of 5427 m^2. Vertical alternation of three UGL beds is visible along several parts of the cliff-platform junction, with the grey marl beds elevated up to 17 m above sea level (asl) on the western side of the platform (Fig. 3a and b).

The overlying softer UGL grey marls also contribute to fine sediment at the cliff-platform junction. The marly cliffs are also vertically chiselled by gullies which transport and deposit boulders and coarse-grained sediments along the cliff-platform junction. Parallel joints, driven by the SE-NW faults in the area, are spaced at intervals ranging between 0.35 m and 1 m and are mostly oriented SW-NE in a cross-shore pattern and shaping the platform into a blocky limestone pavement (Fig. 3c). The joints have also channelled seawater infiltration at subterranean levels, weakening parts of the platform by solution weathering. In some parts of the platforms, it led to the partial collapse of the limestone surface and the creation of an inland basin filled with collapsed boulders (Fig. 3d).

Stepped rugged profiles at Ponta tal-Qammieħ, have develop from outcrops of hardground (Terminal Lower Globigerina Limestone Hardground) and/or conglomerate phosphorite beds (Lower Conglomerate, C1, bed) found between LGL and MGL (Fig. 2a and b).

The shore platform at Ponta tal-Qammieħ has a total surface area of 3435 m^2. Its longest cross-shore profile, from the cliff-platform junction to the seaward end, is 215.2 m and oriented at 260° (WSW). The platform is directly exposed to the NW winds and is within a relatively shallow bathymetric zone of c. >3 m. The highest elevation is c. 4 m asl. The platform dips in a north-easterly direction with a gradient of 5° from the low landward cliff edge, which then gradually decreases to 3° at the northern end (Fig. 2a). The platform is backed by steep-profile cliffs in MGL that increase in elevation from 9 to 15 m in a north-easterly

Fig. 2. Blata l-Bajda shore platform: a. Site view of the shore platform; b. Cliff-platform area in yellow lower band, transitioning into grey middle band in Upper Globigerina Limestone; c. Hummocky foreshore area of the shore platform; d. Collapsed salinas on the shore platform. (For interpretation of the references to colour in this figure legend, the reader is referred to the web version of this article.)

direction (Fig. 2b), in line with the closest fault in the area trending ENE-WSW with an SSE downthrow.

The planar development of the C1 bed on the platform is not uniform in thickness. It is thicker in the seaward direction and decreases towards the backshore area, where the Terminal Lower Globigerina Limestone Hardground (TLGLHg) outcrops in the upper central parts of the platform. This has influenced the surface roughness of the platform, with more rugged sharp mounds and flat-depressions in the front and mid sections of the platform (Fig. 2b) and relatively smoother surfaces at the backshore, where the thickness of the bed is less than c. 2 cm and MGL is more exposed in closer proximity to the cliff-platform junction. The combination of this lithological characteristic and the environmental setting with front and mid sections of the platform more exposed to wave actions from the north-west and north-east, have resulted in the development of a dark, heavily karstified foreshore with numerous flat-floored solution pools and solution-pitted surfaces.

4. Materials and methods

4.1. Traversing micro-erosion meter measurements

Twelve TMEM bolt sites were installed on each shore platform, where possible, along two cross-shore profiles with three bolt sites, each positioned as seaward, middle and landward along each profile at supratidal levels (Fig. 4). Each TMEM bolt site consisted of three titanium bolts (Fig. 4a): two round-headed ones (Model L26 no. 50) and one flat-headed (Model L24 no. 25). TMEM bolt sites were coded as MBB 1–6 for Blata l-Bajda platform (Fig. 4b) and MPQ 1–6 for Ponta tal-Qammieħ (Fig. 4c). Codes 1 and 4 represented seaward bolt sites, 2 and 5 were middle bolt sites and 3 and 6 corresponded to landward bolt sites. This cross-shore sampling method has been used previously in other studies to identify any spatial variation in surface erosion rate with increasing distance from the shoreline (e.g., Robinson, 1977; Gill and Lang, 1983; Kirk, 1977; Porter et al., 2010a; 2010b). The TMEM has a digital dial indicator equipped with an electronic dial gauge and the readings can be directly recorded on a laptop computer. The electronic dial gauge has a resolution of 0.001 mm, a manufacturing accuracy of ±0.003 mm and a range of 12.7 mm. A total of 22 equidistant individual readings (apart at c. 15 mm) within each bolt site were collected every three months to represent one measurement dataset for each bolt site. Erosion rates are denoted in mm/year, with a negative value indicating surface lowering and a positive value representing surface rising. Nine measurement sets, from 21st March 2014 to 29th June 2016 were recorded for calculating erosion and which generated 108 measurement datasets in total (see Table 1).

4.2. Spatial analysis of erosion data

Although 'absolute' erosion rates may be different between bolt sites across a platform surface, such measurement values would reveal little about the differential erosion between the individual measured points across the bolt site surface. In contrast, using the average of the differences between erosion rates at individual points within the bolt site provides information about the relative change in erosion rates between points and over various spatial scales within a bolt site. This indicates if differential erosion between individual points is constant, or whether the average difference increases or decreases as distance between points changes. If variations are revealed, then conceptual models can be confirmed and used to characterise the spatial nature of erosion trends more broadly across the platforms. Fig. 5 illustrates the difference in comparing erosion rates. In example A, the difference of interest is the difference in erosion rate at the same point over time. This is the manner in which erosion rates at point within a TMEM site are usually reported. In example B the difference between erosion rates at point A can be compared to erosion rates at two points close it, i.e. points B and C, for *the same measurement period*. For point A we could then calculate the average difference in erosion rates between that point (A) and the other two points (B and C). This would give us the average difference in erosion rates for that point, point A. We could do the same for points B and C and so obtain the average difference in erosion rates for points A, B and C relative to the points close to them. In example C this idea has been extended so that, for the same measurement period, the average difference between the erosion rate of point A can be calculated for points close by (i.e. points B and C), as well as for points further away, i. e. points D and E. Likewise, we could undertake the same calculation for points B–E to obtain the average difference between erosion rates for all points relative to points close to and increasingly distance from them. We can then use this information to undertake geostatistical analysis of these spatial differences.

Identifying and quantifying these trends across space requires the use of geostatistical analysis. Geostatistical analysis can be employed to explore how erosion rate over the platform surface varies with spatial scale and thus whether erosion measurements are dependent or inde-

Fig. 3. Ponta tal-Qammieħ shore platform: a. Site view of the shore platform; b. Bioturbated surfaces across the platform in stratigraphy of Lower Conglomerate (C1) bed, Terminal Lower Globigerina Limestone Hardground (TLGHg) and Lower Globigerina Limestone (LGL), backed by soft cliffs in Middle Globigerina Limestone (MGL).

pendent of each other. Often this rests on calculating semivariance, which is a measure of how data are related with distance (spatial autocorrelation), recognizing that observations close together in space are more likely to be correlated than those further apart. The semi-variance function, $\delta(h)$, is given as half the average squared difference between data values that are separated by a distance h (Matheron, 1963):

$$\gamma(h) = \frac{1}{2[n(h)]} \sum_{n(h)} (z_i - z_j)^2 \tag{1}$$

where: $n(h)$ refers to the number of distinct pairings of observation, z, at locations i and j and separated by common Euclidian distance h.

This formulation may be applied to data pairings in all directions or further constrained by a range of direction. By plotting semivariance against distance, the semivariogram graph illustrates the nature of the spatial autocorrelation and is used widely in the physical sciences (e.g., Clifford et al., 2005). The trend depicted as semivariance increases with distance reveals how the variable investigated is intrinsically related to spatial scale (variation increases as measurement points move further apart) and might reach an upper limit representing random variance at a distance (the range) at which data are no longer autocorrelated. The majority of semivariogram model structures are monotonic increasing but the shape of the curve, whether linear or non-linear, can vary markedly. However, non-monotonic relationships are also plausible outcomes and may either reveal a near homogeneous spatial domain or depict cyclic patterns ('hole effect' variograms) that could potentially reflect multiple common features located within the total spatial distance plotted (e.g., for an erosion surface, such a pattern might be indicative of multiple erosion foci distributed rather evenly in space and exhibiting similar characteristics).

Here, we define and apply an alternative measure of spatial auto-correlation, $\delta(h)$ as the mean absolute difference between observations

in each pairing over distance h:

$$\delta(h) = \frac{1}{n(h)} \sum_{n(h)} |z_i - z_j| \tag{2}$$

The advantage over the semivariance is that $\delta(h)$ has the same units as z, which is convenient for interpretation, although sacrifices the exaggerating effect generated by squaring the differences between observations in $\delta(h)$. Similar to the semivariogram, plotting $\delta(h)$ as a function of h suitably characterizes the omni-directional spatial continuity of a data set and the type and strength of the spatial dependence.

Here, calculation of $\delta(h)$ and corresponding Euclidian distance, h, for each possible data subset, $n(h)$, over the gridded observation space of interest is performed in a VBA macro in Microsoft® Excel® (Appendix 1). The total number of data pairings included in the analysis is 0.5 $(n^2 - n)$, where n is the number of erosion measurements. A cut-off of 1.4 mm distance between points was identified as at 1.5 mm distance the number of point pairs being measured dropped from 8 to 2.

Erosion rates for individual points within bolts sites are provided in the supplementary information for this paper along with the Excel macro mentioned below. Within this supplementary data, the X and Y co-ordinates of each measurement points are included so that re-searchers can examine the spatial variability of the data or undertake analysis of the differences in erosion rates between measurement points using the Excel macro. The processed data used for curve fitting as well as the curves themselves can be found in the supplementary data associated with this paper. Statistical analyses with linear and quadratic regression tests, in order to determine the relationships between bolt sites was undertaken using SPSS27.

4.3. Conceptual models

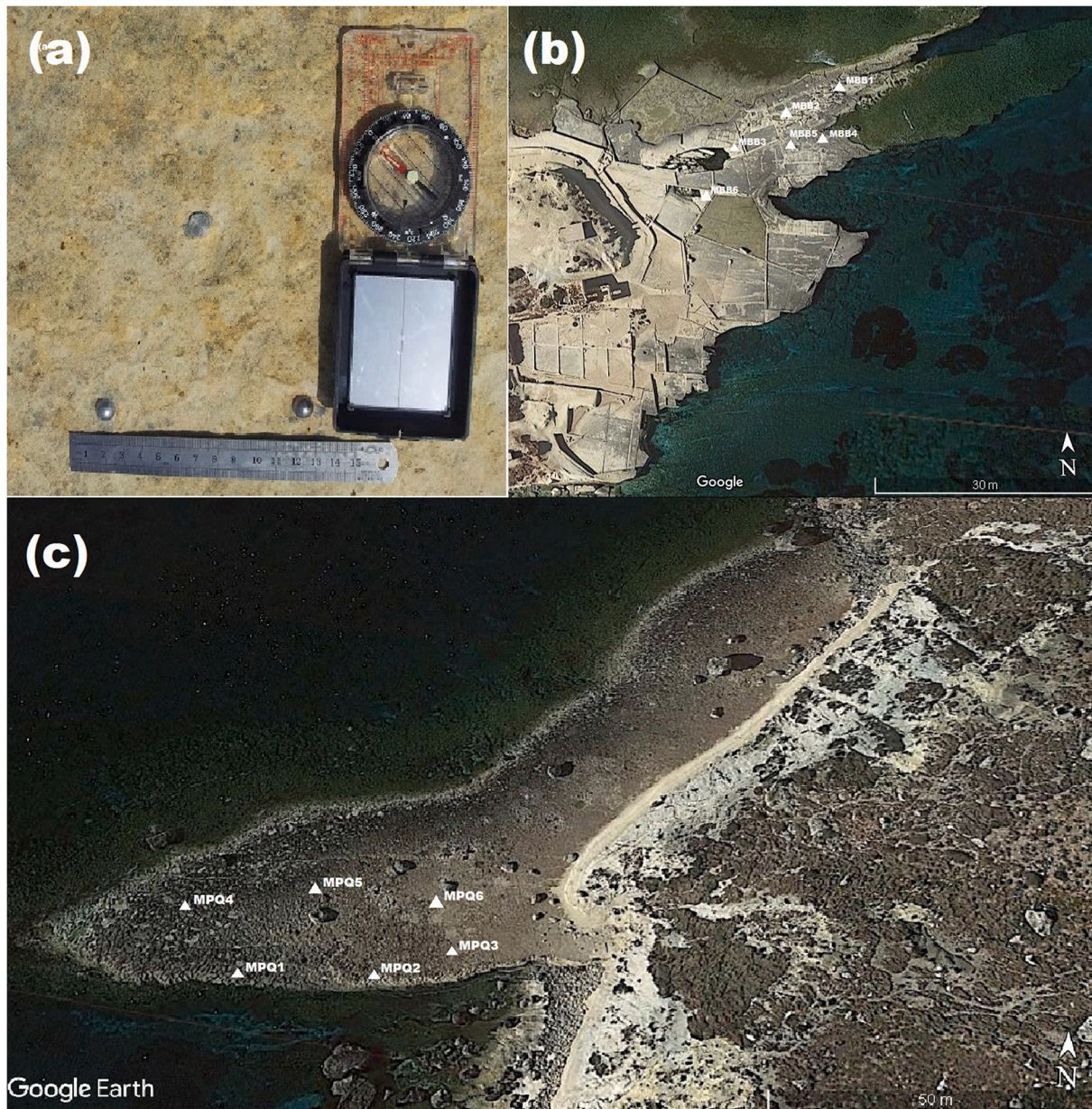We propose and develop simple conceptual models of expected

Fig. 4. Transversing Micro-Erosion Meter (TMEM) stations: a. TMEM station MBB 6 (backshore) on Blata l-Bajda shore platform; b. Location of TMEM stations on Blata l-Bajda shore platform; c. Location of TMEM stations on Ponta tal-Qammieh shore platform.

changes in surface topography that can be identified through an analysis of variations in average erosion rate differences between measurement points on the rock surface. As we are dealing with absolute difference between average erosion then the relationships will always be expressed in positive values.

Fig. 6 illustrates six conceptual models of change in average difference in erosion rates within a hypothetical site. In Model A there is no change in average difference in erosion rates as the distance between points increases. This means that the whole surface across the site behaves, or responds, as a single unit in terms of erosion rate. In Model B, there is an increase with average difference in erosion rates as the distance between points increases. This signifies that differences in average erosion rate diverge between points as distance increases. In Model C, the average difference in erosion rates decreases with the distance between points. This means that the differences in average erosion rates converge across the surface with more distant points, increasingly exhibiting similar rates of erosion. In Model D, whilst in Model E, the

reverse is the case. Models D and E represent situations where intra-site variability is so great that the erosional behaviour completely changes as distance increases between points, initially with rates converging, then diverging (Model D) or initially diverging, then converging (Model E), as illustrated in Fig. 7. The final model, Model F is not shown on the figure as this is the model of no pattern. This is where the there is no clear trend to the average erosion rate differences and so it is not possible to classify the trend. Although this model is not discussed in detail below, it is a model that is common in the analysis. The lack of a trend identifiable with this data does not necessarily mean that there are no spatial trends at these sites. It maybe that the spatial correlations between erosion rates at points operate at a higher resolution than can be detected by the measurements taken in this research. Alternatively, the lack of spatial trends may indicate that each point, at the scale measured in this research, behaves independently of the points around it. This would be of great interest for erosional research as well as it would imply that each set of erosional agents cause changes in erosion rates at each
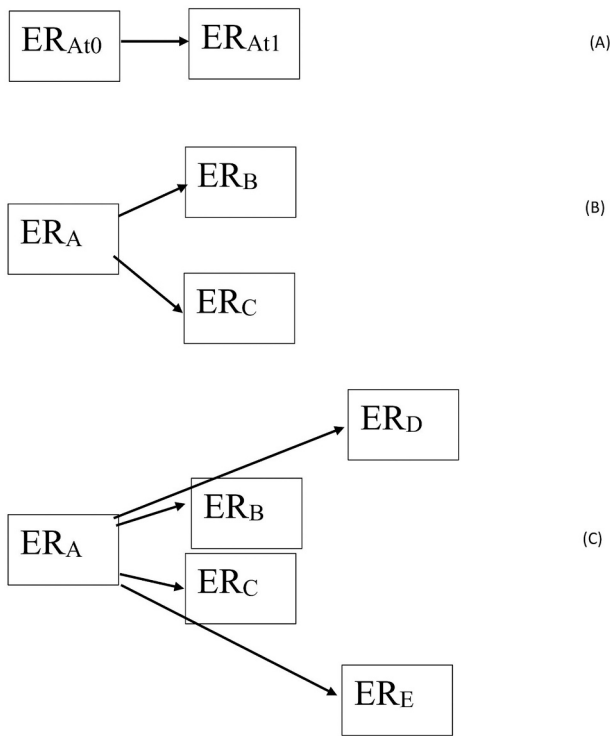
Fig. 5. A simplified visual example of how difference in erosion rates between individual points is calculated according to spatial distance.

measurement points that are unrelated to changes in erosion rates at other measurement points no matter how close they are to each other.

Consistency in the model that most closely describes the change in average erosion rate of measurement points with distance over time at a subject site would imply that there is a consistent and time invariant relationship between the measurement points and their change for the subject site. Variations in the model that describes this relationship at a subject site through time would suggest that relationships between erosion rate at measurement points are subject to change and implies that different processes through time could be affecting these relationships.

The initial form of the topography may be a great influence on the distribution of differences between erosion rate within a measurement site. The 'inheritance' aspect of erosion rates measured at a point has been relatively little researched (Inkpen et al., 2004). If the underlying surface topography has a specific form as outlined in the five models, then this might constrain the nature of erosion rates across each bolts site, forcing them into a pattern similar to that of the underlying topography. Using the same analysis method, we explore how the form of the initial surface may affect (or not) subsequent erosion.

5. Results

The average erosion rates for each bolt used on each platform are presented in Table 2.

Using this alternative measure of spatial auto-correlation we can begin to identify the conceptual models based on the expected trends from this analysis. Undertaking linear and quadratic regression analysis, the equations outlined in Tables 3 and 4 were obtained. Using a F-test of overall significance of the regression analysis enabled the assessment of whether the use of regression analysis provides a better model that fits the data than a model with no independent variables. In Tables 3 and 4, the statistical significance of the regression analysis is indicated for $\alpha = 0.1, 0.05$ and 0.01. Usually $\alpha = 0.05$ or 0.01 is used as an appropriate level of statistically significance, however, for this analysis we have focused on $\alpha = 0.1$ as an appropriate level of statistical significance. The alpha value represents the likelihood of making a Type 1 error, of rejecting the null hypothesis when it is correct, in the case of this research identifying a trend when there isn't one. Another interpretation of the *p* value is that it characterizes the evidence in the data against the null hypothesis. With the data available we felt that a more 'lenient' *p* value for assessing statistical significance was appropriate. The key reasons for this are, firstly, the number of points for each site was relatively low and so it would be expected that the ratio between information identifying a trend as opposed to noise in the data would be relatively high and so a more stringent *p* value might miss information relating to a trend. Secondly, the data used were collected to answer a different set of research questions (see Gauci, 2018) and so the research design was not specifically aimed at answering the research question in this paper. In these circumstances, an alpha value of 0.1 was felt to be justified to extract information for the dataset. It is noted by the authors, however, that applying an alpha value of 0.05 would alter the number of
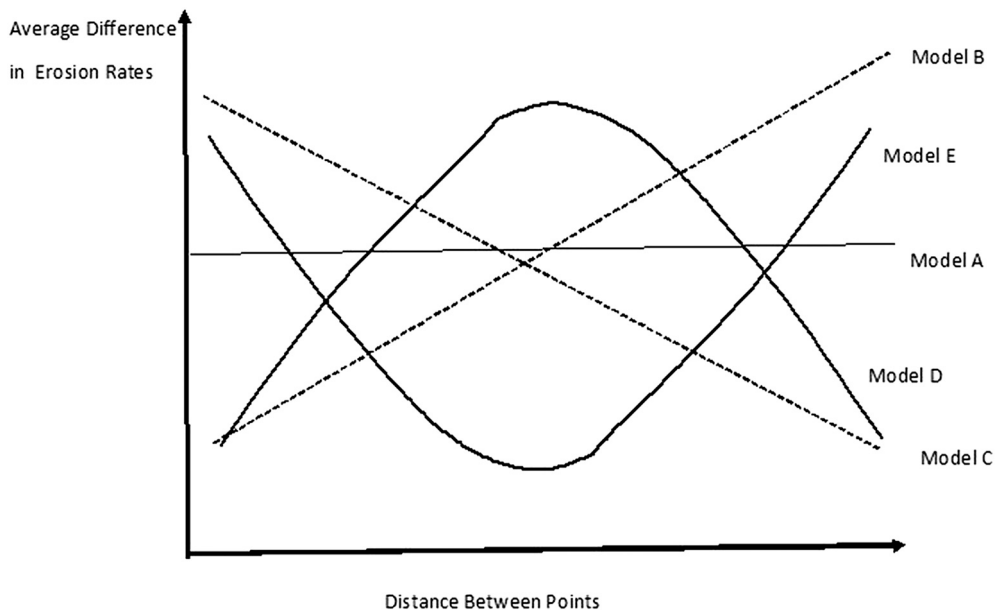

Fig. 6. Model relationships between average difference between erosion rates and distance between measurements points.
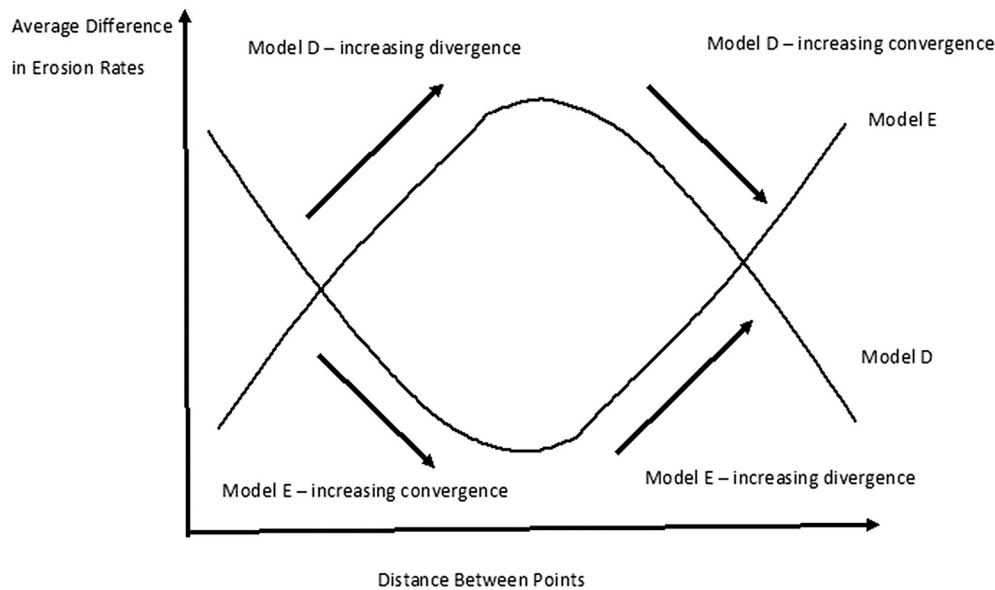
Fig. 7. Convergent and divergent behaviour of differences in average erosion rates as distance between measurements points increases in Models D and E.

Table 1

Measurement periods used for data analysis in paper.

Measurement date	Measurement cycle	Difference between cycles (days)
21st March 2014	1	
13th August 2014	2	156
24th November 2014	3	125
19th March 2015	4	103
12th June	5	100
4th September 2015	6	81
26th December 2015	7	87
29th March 2016	8	120
29th June 2106	9	82

Table 2

Average erosion rate at bolts sites at Blata l-Bajda and Ponta tal-Qammieħ (mm per year) during the study period. Please note: MPB6 was lost during the study period and so the data was not included.

Bolt sites	MPB1	MPB2	MPB3	MPB4	MPB5
Measurement period					
1st–2nd	−0.204	−0.101	−0.089	−0.340	−0.271
2nd–3rd	−0.344	−0.244	−0.106	−0.426	−0.301
3rd–4th	−0.069	−0.188	−0.224	−0.145	−0.163
4th–5th	0.696	−0.080	0.639	0.681	0.633
5th–6th	−1.203	0.742	−1.091	−1.217	−1.195
6th–7th	0.811	−1.095	0.572	0.778	0.829
7th–8th	−0.127	−0.025	−0.074	−0.182	−0.157
8th–9th	−0.133	−0.158	−0.099	−0.153	−0.022

Bolt sites	MPQ1	MPQ2	MPQ3	MPQ4	MPQ5	MPQ6
Measurement period						
1st–2nd	0.272	0.116	−0.199	0.457	0.101	0.025
2nd–3rd	−0.362	−0.124	−0.189	−0.254	−0.400	−0.368
3rd–4th	−0.142	−0.040	0.058	−0.763	−0.128	−0.166
4th–5th	−0.140	−0.157	−0.072	−0.028	−0.090	−0.072
5th–6th	−0.093	−0.141	−0.015	−0.008	0.074	−0.005
6th–7th	0.744	0.177	0.950	0.834	0.919	0.897
7th–8th	−0.263	−0.247	−0.134	−0.027	−0.123	−0.126
8th–9th	−4.348	−1.420	−1.113	−1.144	−1.178	−1.114

relationships identified as statistically significant.

It can be seen that nearly half the measurement periods exhibit statistically significant adherence to the curves representing the different models outlined (Tables 5 and 6). This suggests that in about half the cases considered, there seems to be an identifiable spatial relationship between reading points and distance when analysing the trends of average difference in erosion rates. Specifically, there is no evidence for the model A within the data, whilst models B and C do occur but in only about 5% of the measurement periods. Models D and E were the most common forms of the relationship: with model D occurring in 9% of the measurement periods and model E occurring in 38% of the measurement periods. This would suggest that, although there is variability in the models describing the relationships between average erosion rates as the distance between points changes, the positive quadratic relationship of model E is the dominant relationship when a statistically significant relationship is identified in the data.

Comparing the models describing the relationship between measurement periods, the same model does not provide an appropriate descriptor of the relationship for every measurement period, and this is the case for all sites. The closest is for bolt site MPQ1, which is described by Model E in all except one measurement period. Moreover, bolt sites vary in the number of statistically significant models present and there appears to be no discernible pattern for measurement periods in terms of the consistency of the models identified. This suggests that it may be measurement period and site-specific factors that are most influential in the relationship between average erosion rate and changing distance between points. Specific spatial and temporal scales therefore complement each other and allow a better comprehension of erosional behaviour (Turowski and Cook, 2017).

Initial surface topographies also show a similar variability in differences in average height with distance from any reading point. For the Blata l-Bajda shore platform, quadratic relationships, both negative and positive, tend to best describe the variation with distance between reading points. At this shore platform, however, most of the relationships are not statistically significant. In terms of the research questions, it is clear that the form of the initial surface micro-topography does not constrain the relationship between the average erosion rates of points as distance increases, as the models of change for average erosion rates can be different from the relationship between the point height of the initial topography and the change of height with distance between points.

Analysis of the relationship between differences in average erosion rates at between one point and others and variation with distance

Table 3
Regression analysis of relationship between difference between average erosion rates between points and distance between points at Ponta il Bajda.

	MPB1	MPB2	MPB3	MPB4	MPB5
Height of initial topography	$-0.88x^2 + 1.35x + 1.14$ (0.44))	$-0.41x^2 + 0.86x + 0.49$ (0.41)	***$0.59x^2 - 0.69x + 0.91$ (0.65)***	$-0.65x^2 + 1.39x - 0.66$ (0.34)	$0.84x^2 + 1.41x + 0.53$ (0.18)
1st–2nd	*$-0.15x^2 + 0.18x + 0.20$ (0.55)*	*$0.07x^2 - 0.08x + 0.11$ (0.53)*	**$-0.09x^2 + 0.12x + 0.09$ (0.73)**	$0.16x^2 - 0.18x + 0.34$ (0.36)	*$-0.05x + 0.71$ (0.50)*
2nd–3rd	$-0.03x^2 + 0.03x + 0.11$ (0.22)	$0.03x^2 - 0.04x + 0.08$ (0.31)	**$-0.02x^2 + 0.01x + 0.05$ (0.71)**	$0.10x^2 - 0.27x + 0.49$ (0.38)	*$0.08x + 0.13$ (0.58)*
3rd–4th	$-0.04x + 0.13$ (0.42)	$-0.082x^2 + 0.26x + 0.12$ (0.33)	$0.06x^2 - 0.09x + 0.12$ (0.34)	**$0.23x^2 - 0.40x + 0.33$ (0.67)**	*$-0.06 + 0.07$ (0.51)*
4th–5th	$-0.04x^2 + 0.01x + 0.15$ (0.39)	**$0.12x^2 - 0.05x + 0.15$ (0.65)**	**$-0.08x^2 - 0.01x + 0.08$ (0.65)**	**$0.19x^2 - 0.19x + 0.17$ (0.94)**	**$0.17x^2 - 0.23x + 0.16$ (0.83**
5th–6th	$0.09x^2 - 0.14x + 0.26$ (0.08)	**$0.40x^2 - 0.43x + 0.19$ (0.96)**	$-0.12x^2 + 0.23x + 0.08$ (0.36)	**$0.29x^2 - 0.36x + 0.32$ (0.65)**	**$0.11x + 0.08$ (0.97)**
6th–7th	$0.02x^2 + 0.02x + 0.13$ (0.21)	**$0.18x^2 - 0.18x + 0.11$ (0.98)**	**$0.3x^2 - 0.21x + 0.3$ (0.87)**	**$0.5x^2 - 0.67x + 0.38$ (0.86)**	$0.27x + 0.09$ (0.24)
7th–8th	$0.02x + 0.14$ (0.05)	**$0.79x^2 - 0.99x + 0.49$ (0.86)**	**$0.33x^2 - 0.34x + 0.31$ (0.93)**	**$0.09x^2 - 0.08 + 0.2$ (0.79)**	$-0.03x + 0.17$ (0.28)
8th–9th	*$-0.13x^2 + 0.12x + 0.18$ (0.54)*	**$1.15x^2 - 1.5x + 0.63$ (0.76)**	$0.02x^2 - 0.04x + 0.13$ (0.02)	$-0.12x^2 + 0.17x + 0.17$ (0.18)	$0.05x^2 - 0.11x + 0.21$ (0.25)

Regression equation with r^2 value in brackets.
Statistical significance of regression relationship.
xxx = Not significant.
xxx = Significant at α = 0.10.
xxx = Significant at α = 0.05.
xxx = Significant at α = 0.01.

Table 4
Regression analysis of relationship between difference between average erosion rates between points and distance between points at Ponta tal-Qammieh.

	MPQ1	MPQ2	MPQ3	MPQ4	MPQ5	MPQ6
Height of initial topography	$0.87x^2 - 1.09x + 1.31$ (0.48)	**$0.75x^2 + 0.91x + 1.33$ (0.74)**	*$0.22x + 0.62$ (0.50)*	*$-2.0x^2 + 3.28x + 0.79$ (0.52)*	$-0.43x^2 + 0.84x + 0.32$ (0.36)	*$-0.27x^2 + 1.08x + 1.178$ (0.44)*
1st–2nd	**$0.24x^2 - 0.23x + 0.28$ (0.86)**	$-0.19x^2 + 0.23x + 0.26$ (0.11)	*$-0.17x^2 + 0.47x - 0.04$ (0.65)*	$-0.01x + 0.18$ (0.04)	$0.01x + 0.05$ (0.10)	*$0.02x + 0.06$ (0.30)*
2nd–3rd	**$0.47x^2 - 0.58x + 0.30$ (0.91)**	$0.08x^2 - 0.12x + 1.02$ (0.06)	**$1.78x^2 - 1.98x + 1.68$ (0.94)**	$-0.02x + 0.12$ (0.10)	**$0.08x^2 - 0.10x + 0.09$ (0.63)**	**$0.59x^2 - 0.58x + 0.37$ (0.87)**
3rd–4th	**$0.14x^2 - 0.16x + 0.17$ (0.85)**	$-0.11x^2 + 0.15x + 0.16$ (0.19)	*$1.37x^2 - 2.1x + 1.45$ (0.49)*	$-0.02x^2 + 0.05x + 0.02$ (0.48)	**$0.05x^2 - 0.05x + 0.03$ (0.74)**	**$0.63x^2 - 0.67x + 0.38$ (0.89)**
4th–5th	**$0.85x^2 - 0.10x + 0.47$ (0.93)**	$-0.03x + 0.35$ (0.03)	**$0.02x + 0.02$ (0.77)**	$0.03x^2 - 0.04x + 0.06$ (0.35)	$0.07x^2 - 0.14x + 0.22$ (0.10)	$-0.09x^2 + 0.11 + 0.1$ (0.41)
5th–6th	*$0.15x^2 - 0.21x + 0.21$ (0.53)*	$0.12x^2 - 0.09x + 0.27$ (0.41)	**$0.18x^2 - 0.17x + 0.11$ (0.90)**	**$0.02x^2 - 0.01x + 0.02$ (0.80)**	$0.10x^2 - 0.21x + 0.29$ (0.22)	$-0.4x^2 + 0.05x + 0.05$ (0.39
6th–7th	**$0.25x^2 - 0.33x + 0.20$ (0.64)**	*$0.16x^2 - 0.25x + 0.23$ (0.50)*	**$0.14x^2 - 0.16x + 0.08$ (0.88)**	$-0.35x^2 + 0.61x - 0.07$ (0.20)	$0.004x^2 - 0.006x + 0.022$ (0.08)	**$0.27x^2 - 0.28x + 0.16$ (0.97)**
7th–8th	$-0.005x + 0.134$ (0.02)	$-0.17x^2 + 0.23x + 0.24$ (0.18)	*$-0.09x^2 + 0.11x + 0.11$ (0.52)*	$-0.39x^2 + 0.68x + 0.02$ (0.18)	$0.01x + 0.11$ (0.10)	**$0.10x^2 - 0.10x + 0.16$ (0.83)**
8th–9th	**$0.71x^2 - 0.83x + 0.50$ (0.90)**	$-0.61x^2 + 0.82x + 0.51$ (0.25)	*$-0.11x^2 + 0.14x + 0.06$ (0.76)*	$0.01x^2 - 0.02x + 0.10$ (0.01)	$0.043x + 0.22$ (0.8)	$-0.03x^2 + 0.06x + 0.10$ (0.03)

Regression equation with r^2 value in brackets.
Statistical significance of regression relationship.
xxx = Not significant.
xxx = Significant at α = 0.10.
xxx = Significant at α = 0.05.
xxx = Significant at α = 0.01.

between points suggests that there are specific modes of change that can be identified. Specifically, changes in differences in average erosion rates are dominated by model E types changes. This suggests that differences in average erosion rates tend to initially decrease moving away from a reading point before increasing again, often within a relatively short distance, after about 5 mm between points. Thus, the average erosion rates of an individual point is likely to be different from the average erosion rates of the points around it. If the difference in average erosion rates from a reading point converge with distance, this would imply that the nature of erosion is becoming increasingly similar in its characteristics. As distance increases, however, the difference in average erosion rates between reading points increases. This implies that erosion rates are diverging as distance increases and, therefore, that erosion is increasingly dissimilar in its expression. The quadratic nature of the relationship suggests that there is a distance between points where convergence is greatest, and the surface erodes as almost as if a single unit, but that this distance is contained within the boundaries of the measurement site. It is noticeable, however, that the gradient and intercept coefficients change between measurements periods at the same sites as well as between sites. This suggests that, although the positive quadratic function is a good descriptor of the relationship in a number of cases, the nature of the relationship and the distance at which convergence is greatest can vary within and between bolt sites across measurement periods.

6. Discussion

Models D and E, the initially divergent and initially convergent

Table 5
Model types by measurement period for Ponta il Bajda.

	MPB1	MPB2	MPB3	MPB4	MPB5
Height of initial topography	F	F	**E**	F	F
1st–2nd	**D**	**E**	**D**	F	**C**
2nd–3rd	F	F	**D**	F	**B**
3rd–4th	F	F	F	**E**	**C**
4th–5th	F	**E**	**D**	**E**	**E**
5th–6th	F	**E**	F	**E**	**B**
6th–7th	F	**E**	**E**	**E**	F
7th–8th	F	**E**	**E**	**E**	F
8th–9th	**D**	**E**	F	F	F

B = increase with average difference in erosion rates as the distance between points increases.
C = the average difference in erosion rates decreases with the distance between points.
D = the difference in average erosion rates increases but then decreases as the distance between points increases.
E = the difference in average erosion rates decreases but then increases as the distance between points increases.
F = no pattern.

Table 6
Model types by measurement period for Ponta-tal-Qammieh.

	MPQ1	MPQ2	MPQ3	MQB4	MQB5	MPQ6
Height of initial topography	F	**D**	**B**	**D**	F	**D**
1st–2nd	**E**	F	**D**	F	F	**B**
2nd–3rd	**E**	F	**E**	F	**E**	**E**
3rd–4th	**E**	F	**E**	F	**E**	**E**
4th–5th	**E**	F	**B**	F	F	F
5th–6th	**E**	F	**E**	**E**	F	F
6th–7th	**E**	**E**	**E**	F	F	**E**
7th–8th	F	F	**D**	F	F	**E**
8th–9th	**E**	F	**D**	F	F	F

descriptions of the differences between average erosion rate between points, appear to provide a relatively good guide to surface change. The two models also have different erosion rates associated with them that are statistically significantly, with Model D having much higher levels of erosion that Model E. At Blata l-Bajda, average erosion rate for model D bolt sites was −0.133 mm/year compared to +0.124 mm/year for model E bolts sites, a difference that was statistically significant at α = 0.01 using a two sample *t*-test, whilst at Ponta tal-Qammieħ, Model D bolt sites had average erosion rates of −0.462 mm/year compared to Model E bolt sites which had an average erosion rate of −0.170 mm/year, again a statistically significant difference at α = 0.01. These data suggest that nature of erosion behaviour at the micro-scale, either with convergence or divergence of average erosion rate between points, produces identifiable and measurable differences in erosion rates at the level of the bolt site in a time period. Where convergent behaviour dominates over short spatial scales, there are relatively low erosion rates, whilst where divergent behaviour dominates over short spatial scales, higher erosion rates are apparent.

Importantly, although these different models of behaviour at the scale of the bolt site seem to be present, there is, apart potentially for MPQ1, a lack of consistency in their presence between measurement periods at any specific bolt site. This suggests that the mode of behaviour of the surface at a bolt site is not static or fixed. Instead, the lack of consistency could indicate that the mode of surface behaviour is determined not by a specific set of 'fixed' controls such as microtopography or microstructural elements of the bolt site, as suggested by Swirad et al. (2019). Instead, erosional behaviour may emerge from the relations between the 'static' setting of the bolt site and the dynamic relations with processes in each measurement period. Where these relations are consistent, then a consistent mode of surface change is observed and measured. When these relations are significantly altered then a different

mode of surface change may become dominant within a bolt site. This could suggest that the controls on the mode of erosion at the scale of the bolt site are dynamic and vary with measurement period across most platforms.

It is important to note, however, that microtopography itself may not be a 'fixed' variable within which erosion occurs. In their study on the influence of biofilms on microtopography, Yuan et al. (2019) undertook Friedman two-way analysis of variance and used the relative height at each measurement co-ordinate ranked against the rank of the previous reading over each 2 h period of the experiment. The analysis suggested that there were significant changes in microtopography for each treatment over the 2-hourly measurement period. This illustrates that microtopography itself can be a dynamic factor and also that analysing the relation between points, as the relative ranking does, provides more information about erosional behaviour than from analysing a single measurement point and it changes alone. Likewise, Gómez-Pujol et al. (2007) identify the rock surface as a dynamic entity in their analysis of short-term changes in surface height over a day. Changes in surface height were potentially related to the drying of lichens on the rock surface over this short time period, but each point was analysed relative to itself rather than relative to others points which would have provided more information on the spatial pattern of this short-term dynamic. How this identification of short-term dynamism in microtopography is scaled up to longer-time scales and its potential influence is relatively understudied. Whether microtopography forms a 'dynamic' or 'static' control at different spatial and temporal scales is an intriguing line of inquiry for future research and one in which the analysis relative changes or difference between points could be an important aspect.

Model F, which is relatively common across the sites analysed provides an interesting counter point to the search for spatial and temporal trends in the data. As mentioned above Model F could indicate there are no spatial trends between measurement points or that these trends operate at a higher spatial resolution than can be assessed using the measurement points in this research. Identifying the large number of occurrences of Model F in the analysis suggests that the potential of higher resolution spatial trends needs to be considered further. Additionally, Model F could indicate that the local, within site, relationships between erosional agents and local contingencies such as microtopography and geological variations, are more dominant in determining the relationships between average erosion rates between points. What could be a source of further research is why the dominance of such local contingencies, as potentially illustrated by Model F, do or do not persist between measurement periods? This again highlights the potentially dynamic nature of the relationship between average erosion rates at points and the local context of the site.

Applying a semi-variogram style analysis to data points at the scale of the bolt site, does provide an indication that the outlined conceptual models operate at some sites. This suggests that there is information within the collective of individual point measurements at the scale of the bolt site that could be extracted to help to identify and understand spatial patterns of variability in erosion. The analysis above seems to suggest that mode of behaviour may be related to specific shore platforms or sections of shore platform and so are, potentially, a characteristic of scales larger than individual bolt sites on specific platforms. This initial observation could be the starting point for further questions such as what characteristics of such platforms result in this consistent pattern or conversely, which characteristics prevent it. Such questions can be identified in TMEM datasets, but such datasets can not necessarily be used to answer these questions. Different research designs and equipment focusing on analysing variations in the microstructure and microtopography of such platforms may be better suited to answering these forms of questions.

The relatively limited spatial coverage of the TMEM compared to SfM may seem to make this form of analysis redundant. In the use of SfM to analyse surface change on shore platforms, Swirad et al. (2019) provide a series of DEMs with a 0.001 m resolution in an area 0.5 × 0.5

m. The relatively low cost set-up for acquiring the data, six cameras on an appropriate frame with appropriate control points was the mid-point in a data collection and analysis process that required initial identification and measurement of ground control points using an UAV survey georeferenced to a LiDAR survey. Post-processing of the data collected, outlined in the supplementary information with the paper, emphasised the importance of key software and a detailed understanding of camera optics and photogrammetric processing principles to enable a high degree of confidence in the final DEMs produced for comparison. The paper highlights that accurate SfM data requires a great deal of research infrastructure, so more than the seemingly simple field process of multiple photographs is required. Large datasets are likely to be a key analytical tool in identifying and understanding surface change on shore platforms, but the simpler, in terms of research infrastructure requirements at least, techniques of TMEM can still produce reliable data on surface change on shore platforms. Exclusion of such techniques on the grounds of more advanced ones being available could also have severe implications for the equitable development of academia as outlined in Inkpen et al. (2020) as well as constrain the nature of research questions and answers developed.

In terms of scale, Swirad et al. (2019) provide novel analysis, at least for shore platforms, of magnitude/frequency relationships for erosion and identify different sizes of detachments as well as the spatial and temporal variability of erosion. As they note this enables them to:

> 'better constrain the mechanisms of erosion through analysis of detachment size and shape and to improve understanding of controls on erosion on the basis of the character and spatial and temporal distribution of detachments.' Swirad et al., 2019, p. 1552.

This is an important observation and one that could not have been made with the TMEM. The range of spatial scale covered by the DEMs from the SfM research means that there is the potential to use magnitude/frequency techniques to identify 'breakpoints' in such figures that can be related to detachment size and potentially to process domains. TMEM analysis operates with far fewer data points and, traditionally, has focused on producing average erosion rates over time or over the limited spatial scale of the bolt site and then assumed differences between bolt sites represent differences across the shore platform. To some extent the Swirad et al., make the same assumption at the scale of the platform as they compare their SfM sites across a platform. Extending the information that can be derived from TMEM data does, however, provide information on the nature of change, the mode of behaviour, at a bolt site of the platform surface. Research questions such as what is nature of surface change at a bolt site could be potentially answered by SfM data in order to confirm or reject and to begin to assess the underlying controls on such behaviour.

Conceptually, scale within TMEM studies has been restricted to understanding single points and their relations to other points within the bolt site. The model surface of which research questions can be asked is relatively coarse. Each point measurement does, however, contain a great deal of information about the behaviour of that point and the surface as a whole (Inkpen, 2011). Analysis of relations between points can begin to identify the emergence of common modes of behaviour as in Inkpen (2011) and as in this paper, as well as potentially divergence of behaviour between points within the bolt site. However, this behaviour need not be consistent across time or even within a platform and TMEM data provides a rapid means to assess the persistent of patterns at the scale of the bolt site. Likewise, DEM analysis can link microtopography to point data and so provide the potential to assess the relations of rates to form, a relatively understudied aspect in TMEM research (although see Stephenson et al., 2010, Inkpen et al., 2010).

The models of behaviour outlined in this paper are capable of assessment at different spatial scales as well. Identification of different models and their association with microtopography as identified within SfM analysis could begin to identify underlying controls on the models and on their spatial extension. This will begin to assess how the scale of

forms on the shore platform is controlled by underlying microstructural controls such as geological contingency and how processes interact with these to produce the resultant erosional forms identified, presumable with their associated variation in erosion rates. The influence of geological contingency on surface erosion of Maltese limestone shore platforms was in fact observed on other platforms by Micallef and Williams (2009) and by Gauci (2018). The TMEM analysis suggests further research questions, such as about the influence of geological controls on microtopography and modes of surface change that other techniques can begin to answer and begins to tease out potential emergent scales of erosion on the shore platform. Similarly, this form of analysis begins to address research questions concerning the spatial and temporal scales at which a surface responds to erosional agents. Despite the relatively low spatial resolution of data points compared to SfM, the TMEM still has the capability identify distinct trends. A higher spatial resolution of points would enable further dissection of these tends spatially and may be able to asses if Model F does indicate a site where there are no distinct spatial correlations between the behaviour of points or whether there are but at a smaller spatial resolution. Importantly, the data used to analyse these patterns was not initially collected for this purpose, suggesting that historic TMEM data could be reanalysed in the same manner asking the same research question of different locations and studies. Such research could begin to collate and assess spatial and temporal patterns of erosion rates at a site scale more generally.

7. Conclusions

The analysis in this paper represents one of the first attempt to use erosion rates within a TMEM site to characterise the nature of erosional behaviour at a subsite scale. Identifying, quantifying and classifying variability in erosional behaviour at this scale could aid the understanding of the surface evolution of shore platforms and enable the identification of anomalous behaviour over shorter time scales. The dominance of Model E in the erosional behaviour at the subsite scale implies that this could be a general mode of surface change on the shore platforms examined. Model E highlights the initial convergence then divergence of average erosion rates between points as the distance between points increases. The quadratic and linear relationships used to describe change in difference between average erosion rates as distance between the individual points changes are not, however, consistently strong and are often not statistically significant.

Although only two limestone shore platforms were considered for this paper, the initial analysis does suggest that there may be sites or measurement periods where the dominance of Model E is reduced and other models of surface change are observed, particularly Model F, 'no pattern'. This could suggest that there is geological contingency affecting the evolution of the platform surface at this scale. Similarly, if the presence of different models is observed at specific time periods and, potentially, across a number of sites, then this may suggest an external driver for some forms of behaviour. Extension of this form of analysis to other shore platforms around Malta as well as reanalysis of existing data sets to assess if these behavioural models can be identified would help in determining the universality of the models and the significance of both geological contingency and external drivers in the model behaviours observed. Additionally, the reanalysis of TMEM data could provide the necessary information which newer techniques such as SfM could benefit from in order to better investigate how scales of forms and rates emerge on shore platforms.

Data availability

The data used in this paper is part of a larger data set collected by Dr. Gauci which is currently being worked upon for publications. The full dataset will be made available once these publications are completed. Individuals can request details about the data related to the shore platforms in this specific paper by contacting Dr. Gauci at ritienne.

gauci@um.edu.mt

Declaration of Competing Interest

The authors have no conflict of interests.

Acknowledgements

Appendix A. Supplementary data

Supplementary data to this article can be found online at https://doi.org/10.1016/j.margeo.2022.106880.

References

Alexander, D.A., 1988. Review of the physical geography of malta and its significance for tectonic geomorphology. Quat. Sci. Rev. 7, 41–53.

Andriani, G.F., Walsh, N., 2007. Rocky coast geomorphology and erosional processes: a case study along the Murgia coastline South of Bari, Apulia — SE Italy. Geomorphology 87 (3), 224–238.

Baldassini, N., Mazzei, R., Foresi, L.M., Riforgiato, F., Salvatorini, G., 2013. Calcareous plankton bio-chronostratigraphy of the Maltese Lower Globigneria Limestone member. Acta Geol. Pol. 63, 105–135.

Biolchi, S., Furlani, S., Devoto, S., Gauci, R., Castaldini, D., Soldati, M., 2016. Geomorphological identification, classification and spatial distribution of coastal landforms of Malta (Mediterranean Sea). J. Maps 12 (1), 87–99. Taylor & Francis.

Carter, N.E.A., Viles, H.A., 2005. Bioprotection explored: the story of a little known earth surface process. Geomorphology 67 (3), 273–281. Elsevier.

Chelli, A., Pappalardo, M., Llopis, I.A., Federici, P.R., 2010. The relative influence of lithology and weathering in shaping shore platforms along the coastline of the Gulf of La Spezia (NW Italy) as revealed by rock strength. Geomorphology 118 (1–2), 93–104. https://doi.org/10.1016/j.geomorph.2009.12.011.

Chelli, A., Pappalardo, M., Pannacciulli, F., 2012. Le piattaforme litorali mediterranee: indagare i processi responsabili del loro modellamento per utilizzarle come indicatori dei paleo livelli del mare. In: D'Angelo, S., Fiorentino, S. (Eds.), Contributi al Meeting Marino, 25–26 Ottobre 2012. ISPRA, Roma, pp. 19–24.

Clifford, N.J., Soar, P.J., Harmar, O.P., Gurnell, A.M., Petts, G.E., Emery, J.C., 2005. Assessment of hydrodynamic simulation results for eco-hydraulic and eco-hydrological applications: a spatial semivariance approach. Hydrol. Process. 19, 3631–3648.

Drago, A., 2009. Sea level variability and the 'Milghuba' seiche oscillations in the northern coast of Malta, Central Mediterranean. Phys. Chem. Earth A/B/C 34 (17–18), 948–970.

Furlani, S., Cucchi, F., Forti, F., Rossi, A., 2009. Comparison between coastal and inland Karst limestone lowering rates in the northeastern Adriatic Region (Italy and Croatia). Geomorphology 104 (1–2), 73–81.

Furlani, S., Pappalardo, M., Gómez-Pujol, L., Chelli, A., 2014. Chapter 7: The rock coast of the Mediterranean and Black seas. Geol. Soc. Lond. Mem. 40 (1), 89–123. https://doi.org/10.1144/m40.7.

Furnali, S., Cucchi, F., Biolchi, S., Odorico, R., 2011. Notches in the Northern Adriatic Sea: genesis and development. Quater. Int. 232, 158–168.

Galea, P., 2019. Central Mediterranean tectonics—a key player in the geomorphology of the Maltese Islands. In: Gauci, R., Schembri, J.A. (Eds.), Landscapes and Landforms of the Maltese Islands. Springer, Switzerland, pp. 19–30.

Gauci, R., 2018. The Identification and Quantification of Surface Change on Limestone Shore Platforms of the Maltese Islands. Ph.D Thesis. University of Portsmouth, Portsmouth, UK.

Gauci, R., Inkpen, R., 2019. The physical characteristics of limestone shore platforms on the Maltese islands and their neglected contribution to coastal land use development. In: Gauci, R., Schembri, J.A. (Eds.), Landscapes and Landforms of the Maltese Islands. Springer International Publishing, Cham, Switzerland, ISBN 978-3-030-15456-1, pp. 343–356. World Geomorphological Landscapes.

Gauci, R., Scerri, S., 2019. A synthesis of different geomorphological landscapes on the Maltese islands. In: Gauci, R., Schembri, J.A. (Eds.), In Landscapes and Landforms of the Maltese Islands. Springer International Publishing, Cham, Switzerland, ISBN 978-3-030-15456-1, pp. 49–65. World Geomorphological Landscapes.

Gauci, R., Schembri, J.A. (Eds.), 2019. Landscapes and Landforms of the Maltese Islands. Springer International Publishing, Cham, Switzerland.

Gianelli, L., Salvatorini, G., Giannelli, L., Salvatorini, G., 1972. I foraminiferi planctonici dei sedimenti terziari dell'arcipelago Maltese. Atti Soc. Toscana Sci. Nat. LXXIX (79), 49–74.

Gill, E.D., Lang, J.G., 1983. Micro-erosion meter measurements of rock wear on the Otway coast of southeast Australia. Mar. Geol. 52, 141–156.

Gómez-Pujol, L., Fornós, J.J., Swantesson, J.O.H., 2006. Rock surface millimetre-scale roughness and weathering of supratidal Mallorcan carbonate coasts (Balearic Islands). Earth Surf. Process. Landf. 31 (14), 1792–1801. https://doi.org/10.1002/esp.1379. John Wiley & Sons, Ltd.

Gómez-Pujol, L., Stephenson, W.J., Fornós, J.J., 2007. Two-hourly surface change on supra-tidal rock (Marengo, Victoria, Australia). Earth Surf. Process. Landf. 32 (1), 1–12. https://doi.org/10.1002/esp.1373.

Inkpen, R., 2007. Interpretation of erosion rates on rock surfaces. Area 39, 31–42.

Inkpen, R.J., 2011. Scale as a relational network in weathering studies. Geomorphology 130, 10–16.

Inkpen, R.J., Stephenson, W.J., 2006. Statistical analysis of the significance of site topography and erosion history on erosion rates on intertidal shore platforms, Kaikoura Peninsula, South Island, New Zealand. Geomorphology 81, 18–28.

Inkpen, R.J., Twigg, L., Stephenson, W.J., 2004. The use of multilevel modelling in evaluating controls on erosion rates on inter-tidal shore platforms, Kaikoura Peninsula, South Island, New Zealand. Geomorphology 57, 29–39.

Inkpen, R.J., Stephenson, W.J., Kirk, R.M., Hemmingsen, M.A., Hemmingsen, S.A., 2010. Analysis of relationships between micro-topography and short- and long-term erosion rates on shore platforms at Kaikoura Peninsula, South Island, New Zealand. Geomorphology 121, 266–273.

Inkpen, R., Gauci, R., Gibson, A., 2020. The values of open data. Area. https://doi.org/10.1111/area.12682.

Kanyaya, J.I., Trenhaile, A.S., 2005. Tidal wetting and drying on shore platforms: an experimental assessment. Geomorphology 70 (1), 129–146. https://doi.org/10.1016/j.geomorph.2005.04.005. Elsevier.

Kirk, R.M., 1977. Rates and forms of erosion on intertidal platforms at Kaikoura Peninsula, South Island, New Zealand. N. Z. J. Geol. Geophys. 20, 571–613.

Marshall, R.J., Stephenson, W.J., 2011. The morphodynamics of shore platforms in a micro-tidal setting: interactions between waves and morphology. Mar. Geol. 288 (1–4), 18–31.

Matheron, G., 1963. Principles of geostatistics. Econ. Geol. 58, 1246–1266.

Mayaud, J.R., Viles, H.A., Coombes, M.A., 2014. Exploring the influence of biofilm on short-term expansion and contraction of supratidal rock: an example from the Mediterranean. Earth Surf. Process. Landf. 39 (10), 1404–1412.

Micallef, A., Williams, A.T., 2009. Shore platform denudation measurements along the Maltese coastline. J. Coast. Res. JSTOR 56 (2), 737–741.

Moses, C.A., 2013. Tropical rock coasts: Cliff, notch and platform erosion dynamics. Prog. Phys. Geogr. 37 (2), 206–226.

Moses, C., Smith, B.J., 1994. Limestone weathering in supra-tidal zone: an example from Mallorca. In: Robison, D.A., Williams, R.B.G. (Eds.), Rock Weathering and Landform Evolution. Wiley & Sons, pp. 433–452.

Moses, C., Robinson, D., Barlow, J., 2014. Methods for measuring rock surface weathering and erosion: a critical review. Earth-Sci. Rev. 135, 141–161.

Moses, C., Robinson, D., Kazmer, M., Williams, R., 2015. Towards an improved understanding of erosion rates and tidal notch development on limestone coasts in the Tropics: 10 years of micro-erosion meter measurements, Phang Nga Bay, Thailand. Earth Surf. Process. Landf. 40 (6), 771–782. Wiley Online Library.

Mottershead, D., 1989. Rates and patterns of bedrock denudation by coastal salt spray weathering: a seven-year record. Earth Surf. Process. Landf. 14 (5), 383–398. Wiley Online Library.

Mottershead, D., 2013. Coastal weathering. In: Treatise on Geomorphology, 4. Elsevier, pp. 228–244. Weathering and soils geomorphology.

Naylor, L.A., Coombes, M.A., Viles, H.A., 2012. Reconceptualising the role of organisms in the erosion of rock coasts: a new model. Geomorphology 157–158, 17–30. Elsevier B.V.

Oil Exploration Directorate, 1993. Geological Map of the Maltese Islands, Sheet 1 and 2 – Malta, Gozo and Comino. Scale: 1:25,000, Office of the Prime Minister, resurveyed by Pedley HM, revised by Debono G, Scerri S, cartographer Simpson C., British Geological Survey, Keyworth.

Pappalardo, M., Cappietti, L., Llopis, I.A., Chelli, A., De Fabritiis, L., 2017. Development of shore platforms along the NW coast of Italy: the role of wind waves. J. Coast. Res. 33 (5), 1102–1112.

Paskoff, R., Sanlaville, P., 1978. Observations géomorphologiques sur les côtes de l'archipel Maltais. Z. Geomorph. 22, 310–328.

Pedley, H.M., 2011. The Calabrian Stage, Pleistocene highstand in Malta: a new marker for unravelling the Late Neogene and Quaternary history of the islands. J. Geol. Soc. 168 (4), 913–926.

Pomar, F., Gómez-Pujol, L., Fornós, J.J., Del Valle, L., Nogales, B., 2017. Limestone biopitting in coastal settings: a spatial, morphometric, SEM and molecular microbiology sequencing study in the Mallorca rocky coast (Balearic Islands, Western Mediterranean). Geomorphology 276, 104–115. Elsevier B.V.

Porter, N.J., Trenhaile, A.S., Prestanski, K.J., Kanyaya, J.I., 2010a. Shore platform downwearing in eastern Canada: Micro-tidal Gaspé, Québec. Geomorphology 116 (1–2), 77–86. Elsevier B.V.

Porter, N.J., Trenhaile, A.S., Prestanski, K., Kanyaya, J.I., 2010b. Patterns of surface downwearing on shore platforms in eastern Canada. Earth Surf. Process. Landf. 35, 1973–1810.

Robinson, L.A., 1977. The Morphology and Development of the Northeast Yorkshire Shore Platform, 23, pp. 237–255.

Said, G., Schembri, J., 2010. Malta. In: Encyclopedia of the World's Coastal Landforms. Springer, pp. 751–759.

Shakesby, R.A., Walsh, R.P.D., 1986. Micro-erosion meter measurements of erosion of limestone, Oxwich Point, Gower: some technical considerations and preliminary results. Cambria 13 (2), 213–224.

Spencer, T., Viles, H., 2002. Bioconstruction, bioerosion and disturbance on tropical coasts: coral reefs and rocky limestone shores. Geomorphology 48 (1), 23–50. Elsevier.

Stephenson, W.J., 1997. Improving the traversing micro-erosion meter. J. Coast. Res. 236–241. JSTOR.

Stephenson, W.J., Finlayson, B.L., 2009. Measuring erosion with the micro-erosion meter – contributions to understanding landform evolution. Earth-Sci. Rev. 95, 53–62.

Stephenson, W.J., Kirk, R.M., 1998. Rates and patterns of erosion on inter-tidal shore platforms, Kaikoura Peninsula, South Island, New Zealand. Earth Surf. Process. Landf. 23, 1071–1085.

Stephenson, W.J., Kirk, R.M., 2000a. Development of shore platforms on Kaikoura Peninsula, South Island, New Zealand Part One: the role of waves. Geomorphology 32 (1–2), 21–41.

Stephenson, W.J., Kirk, R.M., 2000b. Development of shore platforms on Kaikoura Peninsula, South Island, New Zealand Part Two: the role of subaerial weathering. Geomorphology 32, 43–56.

Stephenson, W.J., Kirk, R.M., 2001. Surface swelling of coastal bedrock on inter-tidal shore platforms, Kaikoura Peninsula, South Island, New Zealand. Geomorphology 41 (1), 5–21.

Stephenson, W.J., Kirk, R.M., 2005. Shore platforms. In: Schwartz, M. (Ed.), Encyclopaedia of Coastal Science, pp. 873–875.

Stephenson, W.J., Thornton, L.E., 2005. Australian rock coasts: review and prospects. Aust. Geogr. 36 (1), 95–115. Taylor & Francis.

Stephenson, W.J., Taylor, A.J., Hemmingsen, M.A., Tsujimoto, H., Kirk, R.M., 2004. Short-term microscale topographic changes of coastal bedrock on shore platforms. Earth Surf. Process. Landf. 29 (13), 1663–1673.

Stephenson, W.J., Kirk, S.A., Hemmingsen, S.A., Hemmingsen, M.A., 2010. Decadal scale micro erosion rates on shore platforms. Geomorphology 114, 22–29.

Stephenson, W.J., Dickson, M.E., Denys, P.H., 2017. New insights on the relative contributions of coastal processes and tectonics to shore platform development following the Kaikoura earthquake. Earth Surf. Process. Landf. 42, 2214–2220.

Swantesson, J.O.H., Moses, C.A., Berg, G.E., Jansson, K.M., 2006. Methods for measuring shoreplatform micro-erosion; a comparison of the micro-erosion meter and the laser scanner. Z. Geomorphol. Suppl.bd 144, 1–17.

Swirad, Z.M., Rosser, N.J., Brain, M.J., 2019. Identifying mechanisms of shore platform erosion using structure-from-motion (SfM) photogrammetry. Earth Surf. Process. Landf. 44 (8), 1542–1558.

Torunski, H., 1979. Biological erosion and its significance for the morphogenesis of limestone coasts and for nearshore sedimentation (Northern Adriatic). Senckenberg. Marit. 11 (3/6), 193–265.

Trenhaile, A.S., 1987. The Geomorphology of Rock Coasts. Oxford University Press, USA.

Turowski, J.M., Cook, K.L., 2017. Field techniques for measuring bedrock erosion and denudation. Earth Surf. Process. Landf. 42 (1), 109–127.

Viles, H.A., 2013. Synergistic weathering processes. Treatise on. Geomorphology 4, 12–26.

Viles, H.A., Naylor, L.A., Carter, N.E.A., Chaput, D., 2008. Biogeomorphological disturbance regimes: progress in linking ecological and geomorphological systems. Earth Surf. Process. Landf. 33 (9), 1419–1435.

Woodward, J., 2009. The Physical Geography of the Mediterranean, 8. Oxford University Press on Demand.

Yuan, R., Kennedy, D.M., Stephenson, W.J., 2018. Hourly to daily-scale microtopographic fluctuations of supratidal sandstone. Earth Surf. Process. Landf. 43 (15), 3142–3151.

Yuan, R., Kennedy, D.M., Stephenson, W.J., Gómez-Pujol, L., 2019. Experimental investigations into the influence of biofilms and environmental factors on short-term microtopographic fluctuations of supratidal sandstone. Earth Surf. Process. Landf. 44 (7), 1377–1389.

Yuan, R., Kennedy, D.M., Stephenson, W.J., Finlayson, B.L., 2020. The multidecadal spatial patterns of erosion on sandstone shore platforms in south-eastern Australia. Geomorphology 371, 107437.

Yuan, R., Kennedy, D.M., Stephenson, W.J., Finlayson, B.L., 2022. The precision and accuracy of measuring micro-scale erosion on shore platforms. Mar. Geol. 443, 106691.